

# Primary Myocardial Dysfunction in Autosomal Dominant EDMD. A Tissue Doppler and Cardiovascular Magnetic Resonance Study

Gillian C. Smith, MSc,<sup>1</sup> Maria Kinali, MD, MRCPCH,<sup>2</sup> Sanjay K. Prasad, MD, MRCP,<sup>1</sup> Gisèle Bonne, PhD,<sup>3</sup> Francesco Muntoni, MD, FRCPCH,<sup>2</sup> Dudley J. Pennell, MD, FRCP,<sup>1</sup> and Petros Nihoyannopoulos, MD, FRCP<sup>4</sup>

Cardiovascular Magnetic Resonance Unit, Royal Brompton Hospital, and NHLI, Imperial College, London, United Kingdom<sup>1</sup>  
Dubowitz Neuromuscular Centre, Hammersmith Hospital, London, United Kingdom<sup>2</sup>  
Inserm U582, Institut de Myologie, G.H. Pitié-Salpêtrière, Paris, France<sup>3</sup>  
Department of Cardiology, Hammersmith Hospital, London, United Kingdom<sup>4</sup>

## ABSTRACT

**Background:** Emery-Dreifuss muscular dystrophy is a genetically heterogeneous form of muscular dystrophy. One form is inherited in an X-linked fashion and is secondary to mutations in the gene encoding the nuclear protein emerin. A more common variant is inherited in an autosomal dominant way (EDMD2) due to mutations affecting the nuclear lamina protein lamin A/C. Typical features of both conditions are relatively mild skeletal muscle weakness, but cardiac involvement develops almost invariably by adult age, including conduction defects, arrhythmias and cardiomyopathy. Thus, early detection of cardiac abnormalities may be important for planning early therapeutic intervention. **Aim:** In this study, we hypothesized that early myocardial dysfunction can be detected by tissue Doppler echocardiography and CMR in unselected patients with the autosomal dominant form of Emery-Dreifuss muscular dystrophy. This would suggest that fibrosis could be implicated in the pathogenesis of cardiac dysfunction in EDMD2. **Methods:** Eight consecutive patients with genetically proven EDMD2 without pacemakers were enrolled in the study and compared to eight age-matched controls. All patients and controls first underwent a comprehensive echocardiographic-Doppler examination, followed by measurement of mitral annular velocities using pulsed tissue Doppler. Color M-mode tissue images were recorded from the parasternal long axis projections to derive Myocardial Velocity Gradients (MVG). Subsequently, all subjects underwent cardiovascular magnetic resonance (CMR) imaging for function, intrinsic myocardial tissue contrast using T1 and T2 weighted spin echo (TSE) for fat deposition and extrinsic contrast (Gadolinium-DTPA late fibrosis imaging). Strain measurements, using harmonic phase imaging (HARP) tagging were also derived. **Results:** Cavity dimensions LV mass and fractional shortening were similar between patients and controls. The overall body mass index was less in patients than in controls ( $14.5 \pm 1.4$  vs.  $18.1 \pm 2.4$  g/m<sup>2</sup>,  $p < 0.002$ ). While systolic MVG were similar between groups, the early diastolic MVG was lower in patients than in controls ( $4 \pm 1.2$  s<sup>-1</sup> vs.  $7.1 \pm 2.7$ ,  $p < 0.02$ ). On CMR, LA and LV, RV volumes were similar between patients and controls. CMR strain patterns, however, showed a significant reduction in inferior wall contractility in patients compared to controls ( $-0.06 \pm 0.02$  vs  $-0.09 \pm 0.03$ ,  $p < 0.05$ ). No patient showed late gadolinium enhancement. **Conclusion:** Patients with EDMD2 have abnormal left ventricular function prior to developing any cardiac symptoms. The absence of myocardial fibrosis, however, by CMR suggests that this functional abnormality may not be secondary to scarring but could precede it. Tissue Doppler echocardiography and CMR are sensitive methods of assessing the presence of myocardial dysfunction prior to the development of any cardiovascular symptoms.

**Keywords:** Muscular Dystrophies, Cardiovascular Magnetic Resonance Imaging, Tissue Doppler Imaging, Myocardial Tagging; Myocardial Velocity Gradients.

Received 28 October 2005; accepted 5 March 2006

Correspondence to:

Gillian C Smith

CMR Department,

Royal Brompton Hospital,

Sydney Street, London SW3 3TT, UK

email: g.smith@rbht.nhs.uk

## INTRODUCTION

Emery-Dreifuss muscular dystrophy (EDMD) is a genetically heterogeneous form of muscular dystrophy (1). The first gene responsible for EDMD to be identified was the emerin gene, located on chromosome Xq28 and encoding for a nuclear envelope protein. More recent studies identified defects in the LMNA gene encoding two other nuclear envelope proteins, Lamins A and C, responsible for both the autosomal dominant and autosomal recessive forms (EDMD2 & EDMD3) (2, 3).

Since the discovery of mutations in the *LMNA* gene, it has become clear that a number of mutations within this gene are responsible for a surprising large series of allelic disorders (4, 5). These include limb girdle muscular dystrophy 1B (LGMD1B) (6), a form of dilated cardiomyopathy with conduction defects (DCM-CD) (7), the Dunnigan-type familial partial lipodystrophy (FPLD) (8), a form of autosomal recessive axonal neuropathy (Charcot-Marie-Tooth disease, AR-CMT2) (9), mandibuloacral dysplasia (MAD) (10), Hutchinson-Guilford and Werner Progeria syndromes (HGPS) (11–13) and restrictive dermopathy (14).

Cardiac involvement is an invariable finding in EDMD2, which usually occurs by the second to third decade of life. This includes atrial and ventricular arrhythmias and conduction defects, followed by complete heart block or atrial paralysis but also affecting the left ventricle directly in the form of dilated cardiomyopathy (15, 16).

Recently, it has become apparent that cardiac involvement in EDMD2 may be more severe than in other forms of muscular dystrophy (17–19). There are only a few previous studies (20) reporting pathological endomyocardial autopsy findings in EDMD2 with unique atrial pathology and adipose tissue infiltration with deposition of antihuman IgG. The investigation of cardiac involvement in EDMD2 has mainly been based on two-dimensional echocardiography (2DE) and 24 hour ambulatory ECG monitoring (17), and it has been postulated that rhythm or conduction disturbances are the primary cardiac involvement in these patients. Tissue Doppler imaging (TDI) has recently been proposed as a sensitive method in detecting myocardial dysfunction in asymptomatic patients with neuromuscular diseases (21, 22), but it has not been used to assess patients with EDMD2.

Cardiovascular magnetic resonance (CMR) has also been used in patients with congenital myotonic dystrophy and reported to identify changes that might suggest the early presence of fibrosis (23).

The aim of our study was to prospectively determine whether atrial or left ventricular dysfunction can be detected in a preclinical stage, which may be the result of fibrotic myocardial changes and accompany or precede the conduction system damage in EDMD2.

## METHODS

Eight consecutive genetically proven EDMD2 patients were enrolled from patients attending the regular outpatient clinics of the Dubowitz Neuromuscular Centre and invited to participate in the study. Patients with a contraindication to CMR, such as cerebral clips, implantable devices and in particular cardiac pacemakers, were not included. As the disease incidence is low and many patients do have implanted pacemakers, the potential study population was correspondingly low.

Six patients were male, and the age range from 7–42 years (mean, 18.5). Table 1 summarises the clinical profiles of the patient group. All patients had muscle weakness associated with mild to severe mobility impairment. Of the patients studied, one was in atrial flutter, and one had right bundle branch block. Patients were asked to undergo detailed echocardiographic imag-

ing and 24 hour ECG at the Hammersmith Hospital and CMR imaging at the Royal Brompton Hospital on separate days for their convenience. The time between scans ranged from two weeks to three months.

An age matched control group was obtained from eight unaffected volunteers. It was not possible to match the controls for body surface area as the patient group had lower body weights than could be found in healthy volunteers.

The study was approved by Hammersmith Hospital and Royal Brompton Hospital ethics committees and informed written consent was obtained from each subject or subject's guardian before entering the study.

## Echocardiography

First, a comprehensive standard echocardiographic examination was performed using a commercially available diagnostic ultrasound system (HDI 5000, Philips Medical Systems, Crawley, UK) with a 4–2 MHz multifrequency transducer and second harmonic imaging capability for better endocardial border detection. LA size and LV dimensions at end diastole and end-systole were measured to provide an overall assessment of LV function. LV end-diastolic wall thickness was measured and used to calculate left ventricular mass using the Devereux formula (24). Cardiac dimensions were corrected for body surface area. Valves and great vessels were subjectively assessed for structural abnormalities.

Doppler blood pool velocities were measured across the mitral valve in diastole to assess diastolic filling from early (E-wave) and late (A-wave) transmitral velocities (25).

From apical projections, pulsed wave Doppler tissue myocardial velocities were measured in systole and diastole at the atrio-ventricular ring level. Samples were taken from the lateral, septal, anterior and posterior walls using apical four and two-chamber projections. These velocities reflect the longitudinal vector of shortening of the myofibrils and provide an estimate of the ventricular function along the longitudinal axis.

From the parasternal long axis view, an M-mode trace was obtained depicting the endo and epicardial boundaries. Onto this trace, a color coded tissue velocity map was superimposed showing spatial and temporal velocity differences during systole and early and late diastole from which myocardial velocity gradients between subendocardium and subepicardium could be calculated, and thus, the radial LV function estimated. The angle of the M-mode beam was aligned to be perpendicular to the myocardium ( $\leq 5$  degrees). Aliasing was eliminated by appropriate PRF settings, and grey scale gains were adjusted to provide clear delineation of the endocardial and epicardial borders. The ECG was continuously recorded in all cases.

Data captured in freeze frame were downloaded onto a PC with specially designed software (HDI Lab Philips Medical Systems, Best, The Netherlands). Myocardial borders (endocardial and epicardial) of the left ventricular posterior wall were defined and traced by an experienced operator. The MVG was definable as the slope of linear regression of myocardial velocity along each M-mode scan line throughout the myocardium (26).

**Table 1.** Clinical and genetic findings for EDMD2 group

	Case 1	Case 2	Case 3	Case 4	Case 5	Case 6	Case 7	Case 8
Age at diagnosis (years)	8	14.8	2.2	22	25	12.5	11.5	41
Age at study (years)	8.6	15	7	25	25	12	14	42
Sex (M/F)	M	M	M	F	M	F	M	M
CK (x increased)	2.5	4	4	5	5	15	15	15
Inheritance	Dominant	Sporadic	Sporadic	Sporadic	Dominant	Dominant	Dominant	Dominant
Mutation	c.98A > G p.E33G	c.265C > T p.R89C	c.1072G > A p.E358K	c.1072G > A p.E358K	c.136A > G p.146V	c.1357C > T p.R453W	c.1357C > T p.R453W	c.1357C > T p.R453W
LMNA gene	Exon 1	Exon 1	Exon 6	Exon 6	Exon 1	Exon 7	Exon 7	Exon 7
Onset of symptoms (years)	1.5	3	1	4	1.5	3	4	4
Course	Stationary	Stationary	Progressive	Slowly progressive	Slowly progressive	Slowly progressive	Slowly progressive	Slowly progressive but rapid after 30 yrs
Maximum functional ability	I	I	I	I	WC	I	I	WD
Severity	+	+	+++	++	++	+	+	++
Wasting	Medial aspect of calves	Distal thinning of both calves	Scapulo-peroneal	Scapulo-peroneal	Scapulo-peroneal	Scapulo-peroneal, medial aspect of calves	Scapulo-peroneal, medial aspect of calves	Mild proximal
Weakness	TF	UL > LL	UL > LL	UL > LL	UL > LL	UL = LL	UL = LL	UL = LL
Contractures	TA	E, TA	TA	E, H, TA	E, H, TA, HS	E, TA	E, TA	E, H, TA
Spine	Mild rigidity	Rigid	Rigid	Rigid	Rigid	Rigid	Rigid	Rigid
ECG	Normal	Normal	Normal	1st degree AV block	Normal	Normal	Normal	Atrial flutter
24 h Holter	Normal	Normal	Normal RR = 0.34 sec	1st degree AV block, RR = 0.36 sec	Normal	Normal	Normal	AV block
Echocardiogram	Normal FS:30%	Normal, FS: 32%	Normal, FS: 38%	Normal, FS: 32%	Normal FS: 32%	Normal, FS:40%	Normal FS: 30%	Normal FS: 35%
FVC (%)	102	71	40	78	74	80	80	31 NIV since 42 yrs

I = Walking independently; WC = Walking with crutches; WD = Walking independently with difficulty; E = Elbow; H = Hips; TA = Achilles Tendon; HS = Hamstrings; UL = Upper Limbs; LL = Lower Limbs; TF = Trunk Flexors; FS = Fractional Shortening; AV = Atrioventricular; NIV = Non-invasive ventilation.

This may be considered equivalent to radial strain rate of the myocardium.

## CMR

The CMR was performed using a 1.5 T scanner (Magnetom Sonata, Siemens AG Medical Engineering, Erlangen, Germany) using front and back surface coils and prospective ECG triggering. Images for all but one patient were acquired during breath-hold. All anatomical imaging was performed using a steady state free precession (SSFP) sequence. Accurate assessment of ventricular diastolic, systolic volumes and left ventricular mass was facilitated using semi-automated segmentation (CMRtools, Cardiovascular Imaging Solutions, London, United Kingdom). Papillary muscles were included in LV mass and subtracted from LV blood pool. Atrial size was similarly measured during full atrial diastole. All cardiac dimensions were corrected for body surface area.

Turbo spin-echo imaging with T1 and T2 weighting with and without fat suppression was used to show the presence of fibrofatty replacement. Axial cuts optimally showing right ventricular myocardium and short axis cuts through the base, mid-ventricle and apex were obtained to exclude the presence of myocardial fat which appears brighter due to increased contrast.

Gadolinium-DTPA was given as a peripheral intravenous bolus (0.1 mmol/kg bodyweight) to test whether fibrosis plays a role in cardiac involvement in EDMD. Contrast enhanced images were acquired using a segmented inversion recovery sequence. Areas of late gadolinium enhancement were to be expressed as a percentage of normal tissue (27, 28).

Magnetic resonance tagging sequences spatially modulate longitudinal magnetization at end-diastole thus creating a grid of tag patterns that when analyzed reveal local and global cardiac motion patterns. The harmonic phase method (HARP) uses the fact that image phase is related to myocardial motion and spatial derivatives are calculated for each pixel to produce displacement maps (29,30). We acquired 2 long-axis and 3 short-axis projections to give good coverage of all myocardial segments depicting longitudinal, radial and circumferential motion. From this data, we calculated minimal principal strain for controls and study patients. Minimal principal strain is defined as maximal shortening parallel to the fibre direction and correlates with circumferential strain patterns.

## Statistics

Descriptive statistics are presented as mean  $\pm$  1 standard deviation. The relationships between sets of continuous variables were examined using unpaired student *t*-test. All tests were two-tailed, and  $p < 0.05$  was considered statistically significant.

## RESULTS

### Clinical characteristics

Table 1 describes clinical findings, genetics and cardiac and respiratory data for the time of the study. All patients carried a heterozygous *LMNA* mutation. The average patient age was

18.5 years  $\pm$  12 (range 7–42). There were 2 females and 6 males. They were all asymptomatic from the cardiac viewpoint, and no cardiac medication or medication for the myopathy was taken. Six patients had normal sinus rhythm with no conduction abnormalities on 24 hour Holter monitoring. One patient was in atrial flutter, while another had first-degree atrio-ventricular block. Musculoskeletal symptoms started at an average age of  $2.75 \pm 1.25$  (range 1–4) years. All patients were ambulant with mild to marked limitation of functional capacity.

The body mass index (BMI,  $\text{g}/\text{m}^2$ ) of the patient group was lower than in controls ( $15.2 \pm 3.43 \text{ g}/\text{m}^2$  vs.  $18.1 \pm 2.4 \text{ g}/\text{m}^2$ ,  $p = 0.076$ ). This was due mainly to the fact that the adults and older children in the patient group had very low body weights. This low body weight was accredited largely to muscle wasting. There was no significant difference between the BSA of the two groups, although the BSA of the patients was below the expected values for age (31).

### Echocardiographic findings (Table 2)

Echocardiographic imaging was optimal in all eight patients with clear endo and epicardial border delineation.

Patients had normal left ventricular function at the time of examination with a fractional shortening ranging from 33–37% (mean 35%). There was no difference between patients and controls for left atrial size, left ventricular size and fractional shortening. Left ventricular mass was similar between patients and controls. There were no differences in LV mass as calculated by echo or CMR ( $63.3 \pm 12 \text{ g}/\text{m}^2$  for echo and  $60 \pm 18 \text{ g}/\text{m}^2$  for CMR,  $p = 0.95$ ). Mitral E and A wave diastolic velocities were similar for both groups as were the annular E to A wave ratios.

Pulsed tissue Doppler velocities were normal in all mitral annular regions and were similar between patients and controls. The mitral E to annular E wave ratios were also normal. Myocardial velocity gradients were similar between patients and controls during systole. The early diastolic gradient was lower in patients than in controls, however, suggesting early myocardial dysfunction ( $4 \pm 1.2 \text{ s}^{-1}$  vs.  $7.1 \pm 2.7 \text{ s}^{-1}$ ,  $p = 0.02$ ).

**Table 2.** Echo derived parameters

Parameter	Patients	Controls	p
Age (years)	18.5 $\pm$ 12	15.1 $\pm$ 11	0.57
BSA ( $\text{m}^2$ )	1.2 $\pm$ 0.3	1.4 $\pm$ 0.3	0.41
LA/BSA ( $\text{mm}/\text{m}^2$ )	24 $\pm$ 6	28 $\pm$ 4	0.38
LV fractional shortening (%)	35 $\pm$ 2	38 $\pm$ 8	0.44
LV mass/BSA ( $\text{g}/\text{m}^2$ )	63.3 $\pm$ 12	63 $\pm$ 19	0.95
Mitral E/A	1.73 $\pm$ 0.3	1.69 $\pm$ 0.5	0.88
Pulsed Tissue Doppler			
Posterior wall systole (cm/s)	0.13 $\pm$ 0.02	0.11 $\pm$ 0.04	0.33
Posterior wall E (cm/s)	0.18 $\pm$ 0.05	0.19 $\pm$ 0.06	0.75
Posterior wall A (cm/s)	0.05 $\pm$ 0.02	0.08 $\pm$ 0.04	0.07
E/Ea	5 $\pm$ 0.67	5 $\pm$ 1.7	0.58
Ea/Aa	4.6 $\pm$ 2.7	2.4 $\pm$ 0.64	0.21
Colour TDI			
Gradient early diastole ( $\text{s}^{-1}$ )	4 $\pm$ 1.2	7.13 $\pm$ 2.7	0.02
Gradient systole ( $\text{s}^{-1}$ )	3.4 $\pm$ 1.14	3.5 $\pm$ 1.07	0.88

**Table 3.** CMR derived parameters

Parameter	Patients	Controls	p
LV end-diastolic volume/BSA (mL/m <sup>2</sup> )	73 ± 15	72 ± 7	0.86
LV ejection fraction (%)	0.72 ± 5	0.72 ± 4	0.78
LV mass/BSA (g/m <sup>2</sup> )	60 ± 18	61 ± 14	1
RV end diastolic volume/BSA (mL/m <sup>2</sup> )	62 ± 18	69 ± 10	0.36
RV ejection fraction (%)	58 ± 11	63 ± 8	0.32
Left atrial volume/BSA (mL/m <sup>2</sup> )	41 ± 25	38 ± 6	0.69
Right atrial volume/BSA (mL/m <sup>2</sup> )	60 ± 28	55 ± 13	0.68
Inferior wall minimal principal strain (%)	-0.06 ± 0.024	-0.09 ± 0.032	0.048

### Cardiovascular magnetic resonance (Table 3)

All patients tolerated the CMR scan. The youngest patient (age 5 years) could not be cannulated via superficial access and therefore could not be given Gd-DPTA. This patient also could not breath-hold necessitating a TrueFISP real-time acquisition sequence. Resolution was not as good as the breath-hold sequences but adequate for boundary definition and planimetry. Good quality breath-hold images were obtained for all but this one patient, slice thickness 5-7mm according to BSA. Another patient had severe spinal contractions, which made breath-holding difficult and had to be brought out of the scanner during the examination due to discomfort. This prolonged overall scanning time but adequate images were obtained with minimal patient stress.

Left and right ventricular ejection fractions were within normal limits for both patient and control groups. Left and right ventricular volumes corrected for BSA were also within normal limits. There was no significant difference between the corrected ventricular volumes between the two groups. Mean left ventricular mass when corrected for body surface area was below the published normal value of 87 ± 12 g/m<sup>2</sup> (32). The corrected mass for the control group was also below the normal range. Some of these differences may be explained by the relative youth of both patient and control samples when compared with the age range of the previously described group (8–55 yrs, mean 28 ± 9 versus 7–42 yrs, mean 18.5, and 6–30 yrs, mean 15). The EDMD2 group did, however, have a particularly low corrected LV mass, which may be further explained by their relative physical inactivity due to mobility limitations. LV mass was similar between the two groups. Right ventricular mass was not measured due to difficulties with reproducibility in children.

The left atrial volume CMR was greater in both patient group and controls compared with previously published data (33). This group did not, however, include the atrial appendages in their volume measurements and used FLASH sequences for their acquisitions. No patient showed areas of late gadolinium enhancement. There was, however, a significant reduction in inferior wall strain as determined by HARP tagging (Fig. 1) at -0.062 ± 0.024 versus -0.094 ± 0.032 in the control group (p = 0.048) (Table 3).

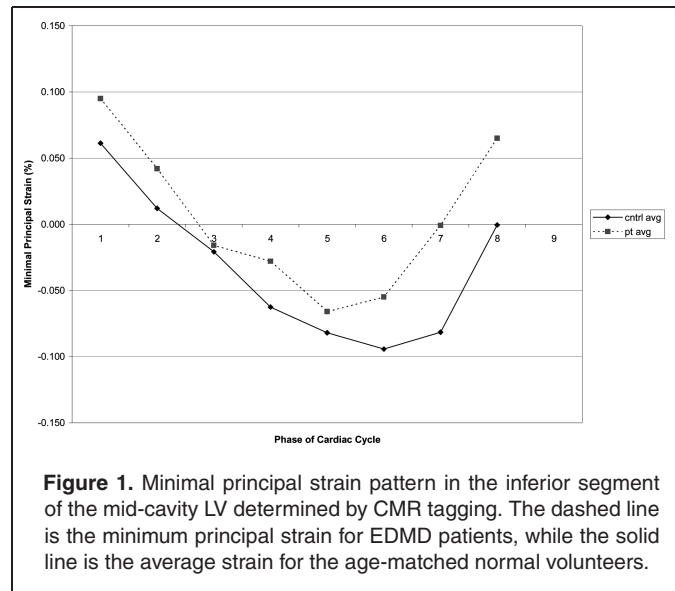


**Figure 1.** Minimal principal strain pattern in the inferior segment of the mid-cavity LV determined by CMR tagging. The dashed line is the minimum principal strain for EDMD patients, while the solid line is the average strain for the age-matched normal volunteers.

### Follow-up

Patients were re-assessed clinically two years after completion of the study. In brief, LV function remained normal overall by conventional echocardiography, but one patient had developed atrial fibrillation.

### DISCUSSION

This is the first study to identify subclinical myocardial dysfunction in consecutive patients with the autosomal dominant form of EDMD. The small series of patient reports available, selected on the basis of specific cardiac abnormalities suggest that the evolution of AV block in the X-linked form seems to evolve slowly, culminating in complete heart block or atrial paralysis for which pacing is indicated to prevent sudden death (36–38). The severity of conduction disturbances appears greater in the dominant form of the disease and ventricular fibrillation may occur. This might explain the relative high frequency of sudden death in this group of patients despite pacing or ICD insertion. Left ventricular dysfunction may occur in the form of apparently isolated dilated cardiomyopathy, especially in EDMD2. One study described 54 living members of one family with a lamin A/C mutation of whom 17 presented with cardiomyopathy and cardiac conduction system disease (15). It is also possible that some individuals undergoing cardiac transplantation for idiopathic cardiomyopathy may in fact have undiagnosed EDMD (39). It is therefore important in this group of patients to risk stratify for pacing/ICD insertion and to predict progressive myocardial disease allowing early pharmacological intervention.

Only one study to date (17) has described the range of cardiac abnormalities in unselected population and found that only 3 of their 10 patients had evidence of ventricular dysfunction on the basis of conventional 2-dimensional echocardiography. Whether EDMD leads primarily to conduction abnormalities as opposed to myocardial fibrosis and dysfunction has remained unknown.

In the current study we hypothesized that patients may develop primary myocardial dysfunction, which will subsequently lead to conduction abnormalities.

TDI been used to describe early changes of myocardial function when conventional echocardiography remains normal (21, 40). The great advantage of TDI is the high frame rate which increases the sensitivity of this technique (41–45). In addition, information on myocardial deformation using the myocardial velocity gradient from subendocardium to subepicardium can be obtained, furthering the assessment of myocardial function. Several groups have reported myocardial abnormalities in sub-clinical conditions leading to cardiomyopathies (21, 22). In this study, early diastolic myocardial velocity gradients were abnormal in a homogeneous group of autosomal dominant EDMD while conventional echocardiography failed to identify any abnormalities.

The most often quoted indices of ventricular function, stroke volume and ejection fraction are unavoidably load and heart rate dependant; therefore, the measurement of ventricular volumes in a non-controlled setting is arguably open to error. While LA dimensions can be measured by echocardiography, CMR can accurately define atrial volumes and function. Interestingly, these were normal by both echocardiography and CMR. Atrial volumes were not increased in comparison to the controls for this patient cohort. This perhaps would refute any primary atrial dysfunction in these patients. Few reports of cardiac muscle pathology in EDMD are available, but myocardial changes with focal degeneration and fatty fibrous replacement have been described (46).

CMR has been used to depict fatty and fibrous infiltration in patients with myotonic dystrophy but not using newer technology including TSE, late enhancement imaging or tagging (47). There was no evidence of late enhancement of the myocardium with gadolinium and no evidence of fibro-fatty replacement using the TSE sequences. There does, however, need to be significant loss of cellular integrity over a macroscopically visible area to detect this. Nevertheless, there was a significant difference in inferior wall strain as determined by HARP tagging suggesting early abnormalities of ventricular function.

Although our patient numbers were limited by the rarity of the disease, these findings support those of other studies of patients with systemic degenerative disease. Studies on patients with Friedreich's ataxia, restrictive cardiomyopathy and athletes have shown that the MVG at early diastole is the most sensitive marker of early changes in myocardial function (21, 26, 40). The relationship between physical immobility and measurements of cardiac function, including MVGs is not established, but this should have no more affect than the opposite phenomenon, athletic training. A recent study has demonstrated a relationship between long-term athletic training and the diminution of age related changes in early diastolic function (40). Our results suggest that cardiac dysfunction precedes significant fibrosis, suggesting that the pathogenesis for the cardiac involvement in EDMD is different from that observed in DMD and BMD. Our results on EDMD2 are in keeping with very recent observations on the cardiac involvement in the animal model with targeted inactivation

of the *LMNA* gene (48). Both CMR tagging and MVG by tissue Doppler consistently showed myocardial dysfunction in the infero-posterior LV wall. Relevant findings in this animal model were early (by 2 weeks of life) cardiac dysfunction with thin-walled, dilated and globular-shaped LV, with a lower mass than in control mice. In similarly aged mice, no evidence of myofibril hypertrophy, necrosis or interstitial fibrosis was found.

Despite the lack of significant histological changes, the contractile properties of single LV myocytes were studied and significantly reduced shortening was demonstrated. At least part of the observed abnormality was related to disruption of the physiological links between desmin at sarcomeres and lamin. Desmin filaments are directly linked between the nuclear surface and the cytoskeleton, and it is possible that lamin contributes to this linkage.

Our data and the experimental animal work favor are an early finding in the process of the disease and therefore a model in which intracellular cardiac defects. This is followed only at a later stage by myocyte loss mostly by apoptosis (48) and eventually fibrosis. This observation has important implication for the understanding of the pathogenesis of the cardiac involvement in EDMD.

### *Clinical implications*

Early detection of myocardial dysfunction in patients with EDMD may necessitate early introduction of ACE inhibition or other treatment in advance of permanent pacemaker implantation. This could delay the latter while reducing or delaying left ventricular remodelling.

### *Study limitations*

Although our study involved a relatively small number of patients, this study is unique in that patients were carefully characterized, genotyped and were selected because they had no evidence of underlying cardiomyopathy and/or pacemakers, while all previous studies involved patients who already had an established cardiomyopathy or conduction system disease. In addition, the fact that so many patients have a permanent pacemaker inserted precluded many from our study, as this currently constitutes a contraindication to CMR. This meant that we were unable to study older patients in whom myocardial abnormality may have been more readily detectable. Pacemakers are now being developed which are more CMR compatible and therefore in the future such patients would not be precluded from CMR.

Myocardial dysfunction was assessed in the anterior septum by CMR tagging and posterior wall using tissue Doppler. This was due to data optimization for both imaging techniques. Nevertheless, abnormalities were found by both, CMR and tissue Doppler suggesting perhaps a diffuse process of myocardial involvement.

## **CONCLUSIONS**

This study suggests that, unlike DMD or BMD, cardiac involvement in EDMD does not appear to involve myocardial

fibrosis in the early stage of the disease. The frequent implantation of pacemakers into patients with EDMD unavoidably restricts the study of a larger patient population, including those with cardiac symptoms. While global systolic function may be normal using conventional echocardiography, there appears to be subtle myocardial abnormalities manifested as a reduction in early diastolic myocardial gradients by echo and systolic strain patterns by CMR. Routine measurement of these may be useful in the early detection of cardiac involvement in EDMD. With further CMR studies, however, with paced patients (49) and the development of MR friendly pacing systems, there is a possibility of ongoing assessment of these patients even post pacemaker implantation.

## ACKNOWLEDGEMENTS

The authors wish to thank Dr. Eugenio Mercuri, Dubowitz Neuromuscular Centre, Imperial College, London; Dr. David Hilton-Jones, John Radcliffe Hospital, Oxford, UK; Dr. Sharmeen Masood PhD, Royal Society/Wolfson Medical Image Computing Laboratory, Imperial College, London, UK; Professor Guang-Zhong Yang, PhD, Director, Royal Society/Wolfson Medical Image Computing Laboratory, Imperial College for the Programming and Analysis of CMR data; and Dr Pascale Richard, UF Myogenetic & Cardiogenetic, AP-HP, G.H. Pitié-Salpêtrière, Paris for their valuable contribution.

## REFERENCES

- Bonne G, Mercuri E, Muchir A, Urtizbera A, Becane HM, Recan D, Merlini L, Wehnert M, Boor R, Reuner U, Vorgerd M, Wicklein EM, Eymard B, Duboc D, Penisson-Besnier I, Cuisset JM, Ferrer X, Desguerre I, Lacombe D, Bushby K, Pollitt C, Toniolo D, Fardeau M, Schwartz K, Muntoni F. Clinical and molecular genetic spectrum of autosomal dominant Emery-Dreifuss muscular dystrophy due to mutations of the lamin A/C gene. *Ann Neurol* 2000;48:170–80.
- Bonne G, Di Barletta MR, Varnous S, Becane HM, Hammouda EH, Merlini L, Muntoni F, Greenberg CR, Gary F, Urtizbera JA, Duboc D, Fardeau M, Toniolo D, Schwartz K. Mutations in the gene encoding lamin A/C cause autosomal dominant Emery-Dreifuss muscular dystrophy. *Nat Genet* 1999;21:285–8.
- Raffaele Di Barletta M, Ricci E, Galluzzi G, Tonali P, Mora M, Morandi L, Romorini A, Voit T, Orstavik KH, Merlini L, Trevisan C, Biancalana V, Housmanowa-Petrusewicz I, Bione S, Ricotti R, Schwartz K, Bonne G, Toniolo D. Different mutations in the LMNA gene cause autosomal dominant and autosomal recessive Emery-Dreifuss muscular dystrophy. *Am J Hum Genet* 2000;66:1407–12.
- Mercuri E, Poppe M, Quinlivan R, Messina S, Kinali M, Demay L, Bourke J, Richard P, Sewry C, Pike M, Bonne G, Muntoni F, Bushby K. Extreme variability of phenotype in patients with an identical missense mutation in the lamin A/C gene: from congenital onset with severe phenotype to milder classic Emery-Dreifuss variant. *Arch Neurol* 2004;61:690–4.
- Wehnert MS, Bonne G. The nuclear muscular dystrophies. *Semin Pediatr Neurol* 2002;9:100–7.
- Muchir A, Bonne G, van der Kooi A, van Meegen M, Baas F, Bolhuis P, de Visser M, Schwartz K. Identification of mutations in the gene encoding lamins A/C in autosomal dominant limb girdle muscular dystrophy with atrioventricular conduction disturbances (LGMD1B) *Human Molecular Genetics* 2000;9:1453–9.
- Fatkin D, MacRae C, Sasaki T, Wolff MR, Porcu M, Frenneaux M, Atherton J, Vidaillet HJ, Spudich S, De Girmami U, Siedman JG, Siedman C, Muntoni F, Muehle G, Johnson W, McDonough B. Missense mutations in the rod domain of the lamin A/C gene as causes of dilated cardiomyopathy and conduction system disease. *New England J Med* 1999;341:1759–62.
- Shackleton S, Lloyd DL, Jackson SN, Evans R, Niermeijer MF, Singh BM, et al. *LMNA*, encoding lamin A/C, is mutated in partial lipodystrophy. *Nat Genet* 2000;24:153–6.
- De Sandre-Giovannoli A, Chaouch M, Vallat SM, Tazir M, Kassouri N, Hammadouche PS, et al. Homozygous defects in *LMNA* encoding lamin A/C nuclear-envelope proteins, cause autosomal recessive axonal neuropathy in human (Charcot-Marie-Tooth disorder type 2) and mouse. *Am J Hum Genet* 2002;70:726–36.
- Novelli G, Muchir A, Sangiuolo F, D'Apice AMR, Massart C, Federici FCM, et al. Mandibuloacral dysplasia is caused by a mutation in *LMNA* encoding lamins A/C. *Am J Hum Genet* 2002;71:426–31.
- De Sandre-Giovannoli A, Bernard R, Cau P, Navarro C, Amiel J, Boccaccio I, Lyonnet S, Stewart CL, Munnich A, Le Merrer M, Levy N. Lamin A truncation in Hutchinson-Gilford progeria. *Science* 2003;300:2055.
- Eriksson M, Brown WT, Gordon LB, Glynn MW, Singer J, Scott L, Erdos MR, Robbins CM, Moses TY, Berglund P, Dutra A, Pak E, Durkin S, Csoka AB, Boehnke M, Glover TW, Collins FS. Recurrent de novo point mutations in lamin A cause Hutchinson-Gilford progeria syndrome. *Nature* 2003;423:293–8.
- Bonne G, Yaou RB, Beroud C, Boriani G, Brown S, de Visser M, Duboc D, Ellis J, Hausmanowa-Petrusewicz I, Lattanzi G, Merlini L, Morris G, Muntoni F, Opolski G, Pinto YM, Sangiuolo F, Toniolo D, Trembath R, van Berlo JH, van der Kooi AJ, Wehnert M. 108th ENMC International Workshop, 3rd Workshop of the MYO-CLUSTER project: EUROMEN, 7th International Emery-Dreifuss Muscular Dystrophy (EDMD) Workshop, 13-15 September 2002, Naarden, The Netherlands. *Neuromuscul Disord* 2003;13:508–15.
- Navarro CL, De Sandre-Giovannoli A, Bernard R, Boccaccio I, Boyer A, Genevieve D, Hadj-Rabia S, Gaudy-Marqueste C, Smitt HS, Vabres P, Faivre L, Verloes A, Van Essen T, Flori E, Hennekam R, Beemer FA, Laurent N, Le Merrer M, Cau P, Levy N. Lamin A and ZMPSTE24 (FACE-1) defects cause nuclear disorganization and identify restrictive dermopathy as a lethal neonatal laminopathy. *Hum Mol Genet* 2004;13:2493–503.
- Becane HM, Bonne G, Varnous S, Muchir A, Ortega V, Hammouda EH, Urtizbera JA, Lavergne T, Fardeau M, Eymard B, Weber S, Schwartz K, Duboc D. High incidence of sudden death with conduction system and myocardial disease due to lamins A and C gene mutation. *Pacing Clin Electrophysiol* 2000;23:1661–6.
- Morris G, Manilal S. Heart to heart: from nuclear proteins to Emery-dreifuss muscular dystrophy. *Hum Mol Gen* 1999;8:1847–51.
- Sanna T, Dello Russo A, Toniolo D, Vytopil M, Pelargonio G, De martino G, Ricci E, Silvestri G, Giglio V, Messano L, Zachara E, Bellocchi F. Cardiac features of Emery-Dreifuss muscular dystrophy caused by lamin A/C gene mutations. *European Heart Journal* 2003;24:2227–33.
- Funakoshi M, Tsuchiya Y, Arahata K. Emerin and cardiomyopathy in Emery-Dreifuss muscular dystrophy. *Neuromuscul Disord* 1999;9:108–14.
- van Berlo JH, Duboc D, Pinto YM. Often seen but rarely recognised: cardiac complications of lamin A/C mutations. *Eur Heart J* 2004;25:812–4.
- Zacharias AS, Wagener ME, Warren ST, Hopkins LC. Emery-Dreifuss muscular dystrophy. *Semin Neurol* 1999;19:67–79.
- Dutka DP, Donnelly E, Palka P, Lange A, Nunez DJR, Nihoyannopoulos P. Echocardiographic characterisation of cardiomyopathy in friedreich's ataxia with tissue doppler echocardiographically derived myocardial velocity gradients. *Circulation* 2000;102:1276–82.

22. Meune C, Pascal O, Becane HM, Heloïre F, Christoforou D, Laforet P, Eymard B, Gueret P, Leturcq F, Recan D, Devaux JY, Weber S, Duboc D. Reliable detection of early myocardial dysfunction by tissue Doppler echocardiography in Becker muscular dystrophy. *Heart* 2004;90:947–8.
23. De Ambroggi L, Raisaro A, Marchiano V, Radice S, Meola G. Cardiac involvement in patients with myotonic dystrophy: characteristic features of magnetic resonance imaging; *Eur Heart* 1995;16:1007–10.
24. Devereux RB, Alonso DR, Lutas EM, Gottlieb GJ, Campo E, Sachs I, Reichek N. Echocardiographic assessment of left ventricular hypertrophy: Comparison to necropsy findings. *Am J Cardiol* 1986;57:450–58.
25. Ommen S, Nishimura R. A clinical approach to the assessment of left ventricular diastolic function by Doppler echocardiography: update 2003. *Heart* 2003;89(Suppl. III):iii18–iii23.
26. Palka P, Lange A, Donnelly J, Nihoyannopoulos P. Differentiation between restrictive cardiomyopathy and constrictive pericarditis by early diastolic Doppler myocardial velocity gradient at the posterior wall. *Circulation* 2000;102:655–62.
27. Kim R, Wu E, Rafael A, Chen E, Parker M, Simonetti O, Klocke F, Bonow R, Judd R. The use of contrast-enhanced magnetic resonance imaging to identify reversible myocardial dysfunction. *N Eng Journal of Medicine* 2000;343:1445–53.
28. Moon J, McKenna W, McCrohon J, Elliott p, Smith G, Pennell D. Toward clinical risk assessment in hypertrophic cardiomyopathy with gadolinium cardiovascular magnetic resonance. *JACC* 2003;41:1561–7.
29. Kuijjer J, Jansen E, Marcus J, van Rossum A, Heethaar R. Improved harmonic phase myocardial strain maps. *Mag Res in Medicine* 2001;46:993–9.
30. Sampath S, Derbyshire J, Atalar E, Osman N, Prince J. Real-time imaging of two-dimensional cardiac strain using a harmonic phase magnetic resonance imaging (HARP-MRI) pulse sequence. *Mag Res in Medicine* 2003;1:154–63.
31. Mosteller R. Simplified calculation of body surface area. *N Eng J Med* 1987;317:1098.
32. Lorenz CH, Walker ES, Morgan VL, Klein SS, Graham TP. Normal human right and left ventricular mass, systolic function, and gender differences by cine magnetic resonance imaging. *Journal of Cardiovascular Magnetic Resonance* 1999;1:7–21.
33. Poutanen T, Ikonen A, Vaino P, Jokinen E, Tikanoja T. Left atrial volume assessed by transthoracic three dimensional echocardiography and magnetic resonance imaging; dynamic changes during the heart cycle in children. *Heart* 2000;83:537–42.
34. Walker S, Levy T, Rex T, Paul V. Biventricular implantable cardioverter defibrillator use in a patient with heart failure and ventricular tachycardia secondary to Emery-Dreifuss syndrome. *Eurpace* 1999;1:206–9.
35. Boriani G, Gallina M, Merlini L, Bonne G, Tonilo D, Amati S, Biffi M, Martignani C, Frabetti L, Bonvicini M, Rapezzi C, Branzi A. Clinical relevance of atrial fibrillation/flutter, stroke, pacemaker implant, and heart failure in Emery-Dreifuss muscular dystrophy: a long-term longitudinal study. *Stroke* 2003;34:901–8.
36. Dreifuss FE, Hogan RG. Survival in X-chromosomal muscular dystrophy. *Neurology* 1961;11:734–7.
37. Wyse DG, Nath FC, Brownell AKW. Benign X-linked Emery-Dreifuss muscular dystrophy is not benign. *PACE* 1987;10:533.
38. Emery A, Dreifuss F. Unusual type of benign X-linked muscular dystrophy. *Journal of Neurology, Neurosurgery and Psychiatry* 1966;29:338–42.
39. Merchut M, Zdonczyk D, Gujrati M. cardiac transplantation in female Emery-Dreifuss muscular dystrophy. *J Neurol* 1990;237:316–9.
40. Palka P, Lange A, Nihoyannopoulos P. The effect of long-term training on age-related left ventricular changes by Doppler myocardial velocity gradient. *Am J Cardiol* 1999;84:1061–7.
41. Nagueu SF, Middleton KJ, Kopelen HA, Zoghbi WA, Quinones MA. Doppler tissue imaging: a non-invasive technique for evaluation of left ventricular relaxation and estimation of filling pressures. *JACC* 1997;30:1527–33.
42. Rambaldi R, Poldermans D, Vletter W, Bax JJ, Roelandt JR. Tissue Doppler imaging and the quantification of myocardial function. *International Journal of Cardiac Imaging* 1998;14:241–50.
43. Sutherland GR, Stewart MJ, Groundstroem KWE, Moran CM, Fleming A, Guell-Peris FJ. Tissue Doppler Echocardiography; historical perspective and technological considerations. *Echocardiography* 1999;16:445–57.
44. Price D, Wallbridge D, Stewart M. Tissue Doppler imaging: current and potential clinical applications. *Heart* 2000;84(Supplement II):11–8.
45. Waggoner AD, Bierig SM. Tissue Doppler Imaging: A useful Echocardiographic Method for the Cardiac Sonographer to Assess Systolic and Diastolic Ventricular Function. *Journal of the American Society of Echocardiography*. 2001;14:1143–52.
46. Yoshioka M, Saida K, Itagaki Y, Kamiya T. Follow up study of cardiac involvement in Emery—Dreifuss muscular dystrophy. *Arch Dis Child* 1989;64:713.
47. Vignaux O, Iazarus A, Varin J, Coste J, Carlier P, Argaud C, Laforet P, Weber S, Legmann P, Duboc D. Right ventricular MR abnormalities in myotonic dystrophy and relationship with intracardiac electrophysiologic test findings: initial results. *Radiology* 2002;224:231–5.
48. Nikolova V, Leimena C, McMahon AC, Tan JC, Chandar S, Jogia D, Kesteven SH, Michalick J, Otway R, Verheyen F, Rainer S, Stewart CL, Martin D, Feneley MP, Fatkin D. Defects in nuclear structure and function promote dilated cardiomyopathy in lamin A/C-deficient mice. *J Clin Invest* 2004;113:357–69.
49. Martin E, Coman J, Shellock F, Pulling M, Fair R, Jenkins K. Magnetic resonance imaging and cardiac pacemaker safety at 1.5-Tesla. *JACC* 2004;43:1315–24.